Bioengineering Single Crystal Growth

Ching-Hsuan Wu, Alexander Park, and Derk Joester*

Department of Materials Science and Engineering, Northwestern University, 2220 Campus Drive, Evanston, Illinois 60208, United States

S *Supporting Information*

ABSTRACT: Biomineralization is a "bottom-up" synthesis process that results in the formation of inorganic/organic nanocomposites with unrivaled control over structure, superior mechanical properties, adaptive response, and the capability of self-repair. While *de novo* design of such highly optimized materials may still be out of reach, engineering of the biosynthetic machinery may offer an alternative route to design advanced materials. Herein, we present an approach using micro-contact-printed lectins for patterning sea urchin embryo primary mesenchyme cells (PMCs) *in vitro*. We demonstrate not only that PMCs cultured on these substrates show attachment to wheat germ agglutinin and concanavalin A patterns but, more importantly, that the deposition and elongation of calcite spicules occurs cooperatively by multiple cells and in alignment with the printed pattern. This allows us to control the placement and orientation of smooth, cylindrical calcite single crystals where the crystallographic *c*-direction is parallel to the cylinder axis and the underlying line pattern.

W hile the production of food, biochemicals, and pharmaceuticals by biotechnological means has reached a high level of sophistication, the development of materials by similar approaches is still in its infancy. Biominerals, for instance, are composite materials with advantageous properties including outstanding mechanical properties and low energy footprint "green" syntheses. However, despite great progress in bio-inspired materials, the ability of organisms to control polymorphs, create smoothly curving yet single-crystalline shapes, and enhance the mechanical properties remains unrivaled.[1,2] Only recently, approaches have been developed to genetically engineer an existing biosynthetic machinery to produce organic/inorganic composite materials with desired shapes, structures, and functionalities. For example, polymorph switching has been demonstrated in zebrafish,[3] and the silica frustules of diatoms have been genetically engineered to function as a mechanically stable, nanoporous support for an enzyme catalyst.[4] One limitation of these approaches is that the number, orientation, or size and shape of the materials cannot be controlled independently. Rather, they are a function of the development of the entire zebrafish and the single-cellular diatom, respectively.

Here we show that sea urchin embryo-derived primary mesenchyme cells (PMCs) grown *in vitro* on micro-patterned cell culture substrates cooperate to create single crystals up to 200 μm in length. This enables the bottom-up synthesis of oriented calcite ($CaCO_3$) single crystals with smooth, cylindrical shape.

In the sea urchin embryo, the PMCs are responsible for synthesizing endoskeletal elements called spicules.[5] Spicules are composites of single-crystalline, magnesium-bearing calcite ($Ca_{0.95}Mg_{0.05}CO_3$) and an organic fraction ($\sim$0.1 wt %) mainly comprised of spicule matrix proteins.[6] Spicule biocalcite is considerably harder, stronger, and more flexible than synthetic calcite,[7] and it displays conchoidal (glassy) fracture rather than cleavage along {104} planes. The biosynthesis of spicules involves transient amorphous calcium carbonate precursors that are thought to be critical in the shaping process.[8]

The PMCs are descendants of the so-called micromeres that arise in the fourth and fifth cleavages of the embryo. During the gastrula stage of embryo development, the PMCs migrate to form a pattern of bilateral symmetry.[9] PMCs then extend processes and fuse their membranes to become a pair of syncytial masses. A calcareous granule is deposited inside the syncytial mass and quickly grows into a rhombohedral prism of calcite. Further growth begins along the crystallographic *a*-directions ("triradial rudiment") and continues along the *c*-direction. The synthesis of the spicules is carried out collaboratively and rapidly (5–13 μm h^{-1}) by the cells contributing to the syncytium[10] and occurs in an environment that is largely sealed off from contact with the outside medium.

PMC migration and patterning has recently been shown to be tightly connected to highly localized expression of vascular endothelial growth factor (VEGF) in the ectoderm.[11] PMCs, however, are autonomous in the actual construction of the skeleton and maintain this ability in culture if a VEGF substitute such as horse serum or matrigel is present in the growth medium during a specific time window.[5]

It is this unusual autonomy that makes *in vitro* cell culture of PMCs possible.[12,13] Because formation and growth of spicules occurs within the syncytial mass, we hypothesized that the growth direction of spicules could be directed by patterning of PMCs *in vitro*. The tripeptide RGD found in numbers of different extracellular matrix (ECM) proteins has been broadly used to promote integrin-mediated cell adhesion and patterning.[14] PMCs, however, are only loosely connected to the basal lamina of the ectoderm,[15] maintain a high degree of motility, and show only slightly enhanced adhesion on fibronectin-coated substrates.[16] In contrast, the lectin wheat germ agglutinin (WGA) binds specifically to oligosaccharides on the surface of PMC,[17] and concanavalin A (ConA) agglutinates micromeres.[18] Moreover, PMCs grown on ConA-treated substrates show a moderate

Scheme 1. Workflow To Control Placement and Orientation of Single-Crystalline Spicules by Micro-Patterned Cell Culture Substrates[a]
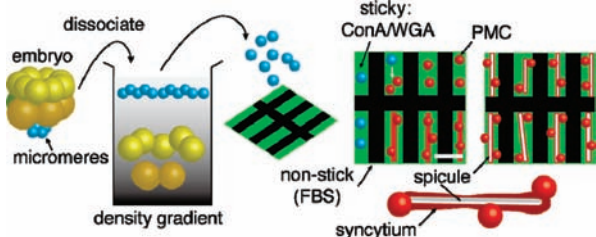
[a] After the fourth cleavage, *S. purpuratus* embryos (created by *in vitro* fertilization) are dissociated. Micromeres (blue) are isolated and placed on the substrates with micro-contact-printed patterns of (fluorescein-conjugated) lectins WGA and ConA (green) on a "nonstick" background (black). In the presence of horse serum, micromeres differentiate into PMCs (red), which attach to the patterns and fuse to form a syncytium. A single-crystalline calcite ($CaCO_3$) spicule is deposited inside the syncytium, in alignment with the underlying lectin pattern.

amount of spreading and reduced mobility.[15] We describe herein the effective use of substrates presenting "sticky" patterns of these lectins on a nonstick background to control spicule deposition.

Micro-patterns of fluorescein-labeled WGA or ConA were transferred onto glass-bottom Petri dishes using micro-contact printing[19] with lectin-inked polydimethylsiloxane (PDMS) elastomer stamps. These substrates were subsequently backfilled with fetal bovine serum (FBS), which discourages PMC adhesion.[17] *Strongylocentrotus purpuratus* micromeres were isolated from the 16-cell larval embryos by established procedures (see Wilt[13] and Supporting Information), seeded onto the lectin-patterned glass-bottom Petri dishes, and cultured in artificial seawater (ASW) at 15 °C for the first 24 h (Scheme 1). During this time, micromeres divide three more times and differentiate into PMCs. Approximately 24 h post fertilization (hpf), the culture medium was changed to ASW containing 2−4% horse serum, which is necessary to trigger spiculogenesis.[13] In the absence of patterns, the *in vitro* behavior of the micromeres and pace of development (i.e., micromere division, PMC development, PMC migration, syncytium formation, spicule deposition, and elongation) are similar to those in the whole embryo, except that *in vitro*-grown spicules are predominantly randomly oriented linear rods, with occasional occurrence of branched structures (Figure 1a).

On both ConA and WGA patterns, PMCs preferentially adhere to the "sticky" lectin patches rather than the FBS-treated substrate up to the mesenchyme blastula stage (22 hpf). On WGA substrates, cells begin to move away from the pattern during the gastrula stage (~40 hpf). In contrast, cells remain on ConA patterns and form syncytia in alignment with the pattern. As a result, the crystalline spicules deposited inside the syncytia show better alignment with ConA after the pluteus stage (~76 hpf). It is currently not clear whether the enhanced mobility on WGA at later developmental stages is a consequence of a loss of the WGA ligands from the cell surface, degradation of the lectin, or deposition of ECM proteins by PMCs.

When micromere-derived PMCs are cultured in ASW (~10 mM Ca^{2+}, ~57 mM Mg^{2+}, pH 7.8−8.4) on an array of parallel ConA lines, the cells primarily deposit spicules with their long axis aligned with pattern (Figure 1b−d). Some spicules form
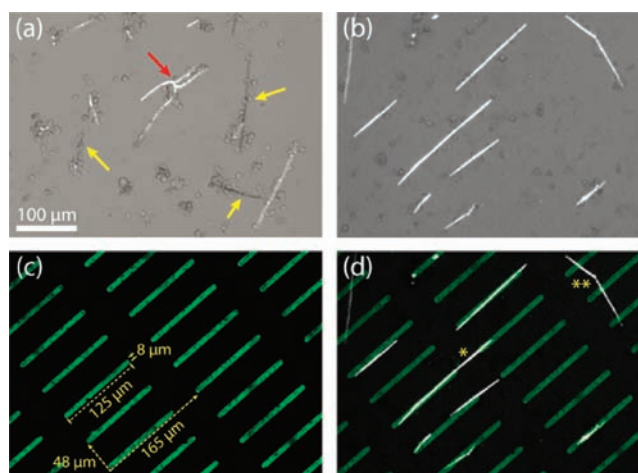

Figure 1. Spicules formed by PMCs on (a) a nonpatterned surface and (b−d) ConA linear array patterns. Entire spicules brighten/extinguish (yellow arrow) as a whole, i.e. are single crystals; branching was occasionally observed (red arrow). (b) Polarized light microscope image showing parallel spicules on ConA pattern. (c) Fluorescent image of fluorescein-labeled ConA pattern (green) on FBS background. (d) Overlay of (b) and (c), showing the spicule-pattern alignment. Bridging can occur along (*) or at an angle (**) to the pattern direction, indicating that cells are able to communicate and/or migrate across the nonstick part of the pattern.

across nonstick regions, forming bridges between separate lectin patterns (Figure 1d). This could be a consequence of PMCs communicating across the divide to form a bridging syncytium or of spicule growth following a preferred direction and "overshooting" the sticky pattern. In either case, the spicule is completely surrounded by the syncytial mass[20] and is not in direct contact with the growth medium or the cell culture substrate. While the medium is likely supersaturated with respect to $CaCO_3$, the nucleation of $CaCO_3$ is very slow under these conditions (~10 mM Ca^{2+}, ~57 mM Mg^{2+}, pH 7.8−8.4) and would be expected to give aragonite at this Mg/Ca ratio.[21] We observed no birefringent material other than the calcite spicules deposited inside the PMC syncytia.

On a square grid pattern, spicules align with either of the orthogonal directions (Figure 2a). The length of spicules follows a log-normal distribution, with a mean at 62.3 μm and a standard deviation of 33.0 μm. The spicule diameter ranges from 1 to 2 μm. The degree of alignment on a square grid pattern (Figure 3) is such that ~40% of spicules are rotated less than $\alpha = \pm5°$ with respect to the grid line, which at a spicule length of ~90 μm corresponds to a deviation of less than one line width (8 μm). More than 64% of the spicules are within $\pm15°$. At least some of the misalignment is due to mechanical perturbation during washing and transportation of the cell culture dishes. In any case, there is a clear trend toward better alignment (small α) for longer spicules (i.e., >90 μm). It is conceivable that this is because syncytia do not form across multiple nonsticky patches or because misaligned spicules cease elongation when the growth tip is too far from a sticky pattern. In order to differentiate between these and other possibilities, we are currently investigating the dynamics of PMC attachment to the printed patterns, syncytium formation, and spicule growth in time-lapse experiments.

After removal of the cellular material with sodium hypochlorite (bleach), the spicule surface appears smooth without displaying any facets when examined by scanning electron microscopy
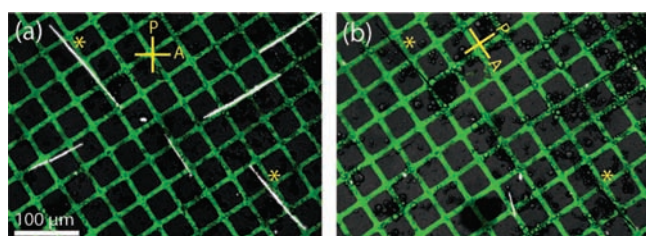
Figure 2. Composites of polarized light and fluorescence microscopy images of spicules (white) formed on a FITC-labeled ConA square grid pattern (green, lattice parameter a = 48 μm; line width d = 8 μm). Spicules brighten and extinguish (*) simultaneously when the sample is rotated between the crossed polarizer (P) and analyzer (A).
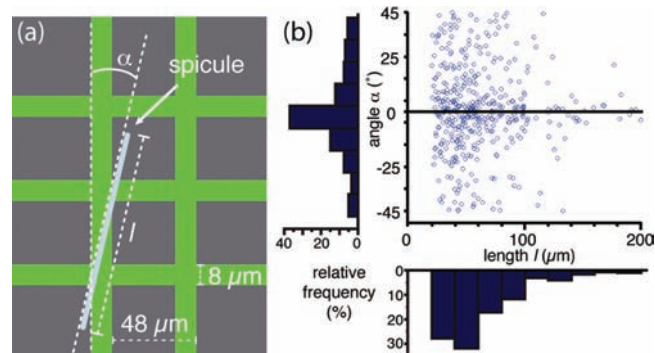

Figure 3. (a) Scheme of the angle α between a spicule and the underlying grid pattern. (b) Scatter plot of the spicule length vs the angle α with corresponding histograms. Note the trend toward good alignment for long spicules.

(SEM, Figure 4). The cross-section of the spicules, as revealed by focused ion beam milling, is circular. However, spicules aligned with the ConA grid pattern alternately brighten and extinguish (when parallel to polarizer or analyzer) as a whole when viewed under crossed polarizers, indicating that each spicule is a single birefringent calcite crystal with its optical axis in a plane parallel to the long axis of the spicule (Figure 2). In overgrowth experiments,[22] stacks of rhombohedral calcite crystals nucleate on spicules. The {104} faces of these rhombohedra are perfectly aligned over the entire length of the spicule (Figure 4c,d). From the orientation of the faces, the edges between them, and the angles that they enclose, it follows that the crystallographic c-axis of calcite almost perfectly coincides with the long axis of the spicule (Figure 4e), which is aligned with the underlying ConA grid line. Small deviations such as the slight tilt (<4°) of the c-axis in the simulated crystal out of the image plane, as apparent by the fact that the a_2- and a_3-axes do not superimpose in the projection, may be a consequence of sample not being mounted perfectly flat with respect to the microscope stage or may result from errors in determining angles accurately.

In conclusion, we demonstrate herein that micro-contact printing of the lectin ConA allows for effective micro-patterning of PMCs. This enables us to control the orientation of smooth, cylindrical rods of single-crystalline calcite deposited by the cell. The orientation of the calcite lattice with respect to the printed pattern is such that the crystallographic c-axis is parallel to the grid lines. Our approach constitutes a biotechnological bottom-up synthesis of oriented single crystals that, among others, may be applied in the design and fabrication of cylindrical lens arrays.
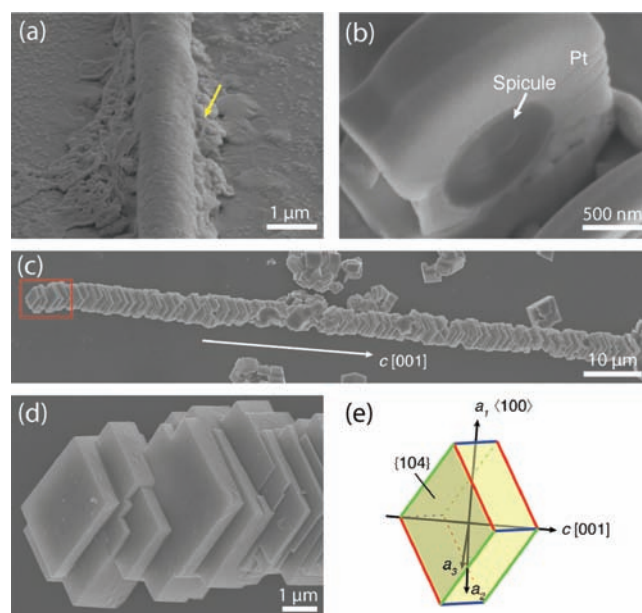

Figure 4. (a) *In vitro*-deposited spicule on a patterned surface after removal of organic material (remnants: yellow arrow) with bleach. Note that the spicule surface does not exhibit facets. (b) The circular cross section of the spicule is apparent after focused ion beam milling a trench through a length of the spicule that was protected against radiation damage by *in situ*-deposited platinum. (c) SEM of a spicule after removal of organic material and overgrown with calcite crystals. The calcite {104} faces are parallel over the entire length of the spicule, indicating the single-crystalline character of the underlying spicule. Several small crystals that nucleated on the cell culture substrate during the overgrowth experiment are also visible. (d) Detail of the boxed region in (c) showing overgrown spicule expressing {104} faces. (e) Simulated calcite rhombohedron bounded by {104} faces, oriented with its faces and edges parallel to those visible in (d). Note that the c-axis is almost perfectly parallel to the long axis of the spicule. (In panel c, the white arrow indicates the line parallel to the c-axis in panel e.)

We envision that micro-patterned PMC culture will furthermore provide a basis for improving our understanding of and control over the cellular machinery responsible for crystal synthesis and ultimately become a platform for biotechnological materials synthesis.

■ ASSOCIATED CONTENT

ⓢ Supporting Information. Soft lithography, cell culture, light microscopy, and SEM. This material is available free of charge via the Internet at http://pubs.acs.org.

■ AUTHOR INFORMATION

Corresponding Author
d-joester@northwestern.edu

■ ACKNOWLEDGMENT

■ REFERENCES

(1) Ji, B.; Gao, H. *J. Mech. Phys. Solids* **2004**, *52*, 1963.

(2) Weiner, S.; Addadi, L. *J. Mater. Chem.* **1997**, *7*, 689.

(3) Sollner, C.; Burghammer, M.; Busch-Nentwich, E.; Berger, J.; Schwarz, H.; Riekel, C.; Nicolson, T. *Science* **2003**, *302*, 282.

(4) Kröger, N. *Curr. Opin. Chem. Biol.* **2007**, *11*, 662.

(5) Wilt, F. H. *Zool. Sci.* **2002**, *19*, 253.

(6) Mann, K.; Wilt, F.; Poustka, A. *Proteome Sci.* **2010**, *8*, 33.

(7) Emlet, R. B. *Biol. Bull.* **1982**, *163*, 264.

(8) Politi, Y.; Metzler, R. A.; Abrecht, M.; Gilbert, B.; Wilt, F. H.; Sagi, I.; Addadi, L.; Weiner, S.; Gilbert, P. *Proc. Natl. Acad. Sci. U.S.A.* **2008**, *105*, 17362.

(9) Okazaki, K. *Embryologia* **1960**, *5*, 283.

(10) Guss, K. A.; Ettensohn, C. A. *Development* **1997**, *124*, 1899.

(11) Duloquin, L.; Lhomond, G.; Gache, C. *Development* **2007**, *134*, 2293.

(12) Okazaki, K. *Integr. Compar. Biol.* **1975**, *15*, 567.

(13) Wilt, F. H.; Benson, S. C. *Development of Sea Urchins, Ascidians, and Other Invertebrate Deuterostomes: Experimental Approaches*; Elsevier Academic Press Inc.: San Diego, 2004; Vol. 74, p 273.

(14) Hersel, U.; Dahmen, C.; Kessler, H. *Biomaterials* **2003**, *24*, 4385.

(15) Lane, M.; Solursh, M. *Dev. Biol.* **1988**, *127*, 78.

(16) Venkatasubramanian, K.; Solursh, M. *Exp. Cell Res.* **1984**, *154*, 421.

(17) Ettensohn, C. A.; McClay, D. R. *Exp. Cell Res.* **1987**, *168*, 431.

(18) Roberson, M.; Oppenheimer, S. B. *Exp. Cell Res.* **1975**, *91*, 263.

(19) Whitesides, G. M.; Ostuni, E.; Takayama, S.; Jiang, X. Y.; Ingber, D. E. *Annu. Rev. Biomed. Eng.* **2001**, *3*, 335.

(20) Beniash, E.; Addadi, L.; Weiner, S. *J. Struct. Biol.* **1999**, *125*, 50.

(21) Morse, J.; Arvidson, R.; Luettge, A. *Chem. Rev* **2007**, *107*, 342.

(22) Okazaki, K.; Inoue, S. *Dev. Growth Differ.* **1976**, *18*, 413.

1661

dx.doi.org/10.1021/ja109500e |*J. Am. Chem. Soc.* 2011, 133, 1658–1661